Desalination and Water Treatment
www.deswater.com

doi: 10.5004/dwt.2017.20444

67 (2017) 389–396
March

Coadsorption of antibiotic amoxicillin and hexavalent chromium from saline water by seaweed-based porous activated carbon

Huihui Gan*, Jiawei Cai, Chang Zhang, Zhengrong Dong, Huixia Jin, Kefeng Zhang

School of Civil Engineering and Architecture, Ningbo Institute of Technology, Zhejiang University, 1 South Qianhu Road, Ningbo 315100, China, Tel. +86-574-88130283; Fax: +86-574-88130283; email: hhgan@nit.zju.edu.cn

Received 11 April 2016; Accepted 15 December 2016

ABSTRACT

The seaweed, kelp was used as a precursor for the preparation of activated carbon by phosphoric acid activation. The effect of heat treatment on the porous and adsorption properties of the prepared activated carbon was investigated by N_2 adsorption–desorption isotherms. Additionally, the coadsorption of antibiotic amoxicillin and chromium from saline water onto the activated carbon from the seaweed was evaluated. The Freundlich isotherms for the adsorption of amoxicillin indicated that the adsorption capacities of the prepared activated carbon from seawater were significantly higher when heat treated at 400°C and 500°C than 200°C and 300°C. On the other hand, for the adsorption of hexavalent chromium, findings were the direct opposite. The adsorption processes of amoxicillin and hexavalent chromium were well described by the pseudo-second-order kinetic model. The optimum pH was around 6.3 for the adsorption of hexavalent chromium in the mixed system containing amoxicillin and hexavalent chromium onto AC400.

Keywords: Amoxicillin; Chromium; Activated carbon; Seaweed; Seawater

1. Introduction

Pollution of coastal waters by heavy metal ions has become an important issue across the world [1–3]. This is because low concentrations of heavy metals in water can cause instability, disorder and harm to living organisms. Among the various heavy metals, hexavalent chromium Cr(VI) is highly toxic to living organisms because of its mutagenic and carcinogenic properties. Antibiotics emerged in aquatic environment are regarded as a serious ecological issue. Many antibiotics are hardly removed even by a sewage treatment that would introduce to the seawater in coastal area [4]. Amoxicillin is a broad-spectrum antibiotic and commonly used due to its high bacterial resistance and large spectrum against bacteria. Additionally, amoxicillin have been reported to be hardly degraded, and its toxic effects can do harm to organisms [5,6]. Heavy metal ions and organic pollutants often coexist in aquatic environments in low concentrations, which aggravate the risk of water quality. Therefore, practical and effective methods are needed to eliminate these complex pollutants [7,8].

Adsorption is an excellent method for the removal of toxic metals and organic pollutants from wastewater, which is known for its flexibility, simple operation, and potential for regeneration and reuse [9]. Activated carbon is an effective and widely used adsorbent, but it remains an expensive material due to the high initial and system regeneration costs [10]. In recent years, increased attention has been focused on the development of adsorbents based on low-cost biomaterials and industrial by-products [11–15]. Many agricultural materials are used as raw materials for the production of activated carbon, including corn hull, rice straw, coconut shell, fruit stones, nutshell and other carbonaceous wastes [16–18]. The diversity of the structure and elemental content of biomass possible leads to the formation of activated carbon with different porous structures [19]. Seaweeds with high carbon content are renewable biomass. The proliferation of the seaweed biomass is ubiquitous and abundant in worldwide littoral zones. Several attempts have

* Corresponding author.

been made to use seaweed as a bioadsorbent [20–22] or the raw material for the development of activated carbon. Green alga *Ulva lactuca* and its activated carbon were reported for the removal of chromium from wastewater [23]. Aravindhan et al. [24] prepared activated carbon from two macroalgal biomass by zinc chloride activation and examined for the removal of phenol from aqueous solution [24] The findings were reported to be promising. It is interesting to note that few studies have investigated the simultaneous removal metals and organic contaminants using activated carbon from seaweeds.

Besides, the types of raw materials, and the surface and porous properties of the activated carbon greatly influence the preparation method and conditions. In general, there are two kinds of processes for the preparation of activated carbon, namely physical and chemical activation [25]. For physical activation, the carbonization initially occurs in an inert atmosphere, and activation of the resulting char follows at high temperatures (800°C–1,100°C) with activating agents. On the other hand, the chemical activation is performed at lower temperatures (400°C–800°C), whereby the carbonization and activation processes proceed at the same time in the presence of chemical agents such as phosphoric acid and zinc chloride. Chemical activation is also better for the development of a porous structure [26,27].

In this work, the kelp, large seaweeds, are used as a precursor for the preparation of activated carbon by phosphoric acid activation. The prepared activated carbon was evaluated in terms of the following: (i) coadsorption properties of antibiotic amoxicillin and hexavalent chromium from saline water; (ii) effects of activation temperature on the porosity and adsorption properties of the prepared activated carbon; (iii) influence of pH on the coadsorption of amoxicillin and hexavalent chromium onto the prepared activated carbon and (iv) adsorption kinetics and isotherm mechanisms.

2. Experimental setup

2.1. Preparation of adsorbent and adsorbate

The seaweed, kelp obtained from the Zhejiang province in China was washed with distilled water to eliminate dust and water soluble impurities. They were then oven-dried at 100°C for 48 h and sieved to obtain particle sizes of less than 0.15 mm (100 mesh) diameter. The kelp particles were activated by phosphoric acid activation [28,29]. The kelp particles were impregnated with H_3PO_4 aqueous solution (20%) for 2 h. Then, the impregnated particles were heat treated in an N_2 atmosphere at 200°C, 300°C, 400°C and 500°C for 3 h, respectively. The heat treated samples were washed with boiled hydrochloric acid solution (0.1 M) for several times and subsequently with distilled water until no phosphate ions were detected in the water and a pH close to that of distilled water was reached. The obtained wet cakes were dried at 100°C for 12 h and ground, which were labeled as samples AC200, AC300, AC400 and AC500 for the different heat treatment temperatures, respectively.

2.2. Characterization of activated carbons

The C, H and N contents (mass%) of the activated carbons were measured by elemental analysis (Flash EA 1112, Thermo Finnigan, America). The N_2 adsorption–desorption isotherms of the activated carbons were measured using an automatic adsorption instrument (ASAP 2020M, Micromeritics, America). The Barrett–Joyner–Halenda method was used to calculate the pore distribution [30]. The micropore volume was calculated with the *t*-plot method [31]. The mesopore volume was calculated as the difference between the micropore volume and the total pore volume.

2.3. Adsorption experiments

The adsorption characteristics of the prepared activated carbons were studied using a mixed system of artificial seawater containing amoxicillin and chromium. The artificial seawater was prepared by adding 35 g of sea salts per liter (Instant Ocean® Sea Salt). The mixed system solution was prepared by dissolving a certain amount of amoxicillin and potassium dichromate ($K_2Cr_2O_7$) in the prepared artificial seawater. All adsorption experiments were carried out on a thermostated shaker (KYC-1102C, China) operated at 170 rpm. Adsorption studies were carried out with 300 mg of activated carbon samples introduced into 100 mL of the mixed solutions of amoxicillin and chromium. The effect of pH on the adsorption of the mixed amoxicillin (200 mg/L) and chromium (2.5 mg/L) onto the AC400 was studied over the pH range of 4.0–7.9. The point of zero charge (pH_{pzc}) analysis was performed by adding 50 mg of the AC400 into 50 mL of 0.01 mol/L KNO_3 solution with initial pH ($pH_{initial}$) values of 2.0–10.0. After in contact at 170 rpm for 48 h, the finial pH (pH_{final}) of the system was measured. The pH_{pzc} was determined from the plot of ΔpH [$pH_{initial}$ − pH_{final}] vs. $pH_{initial}$. Solution pH was adjusted with HNO_3 and NaOH solutions (1.0 mol/L).

The adsorption isotherms of amoxicillin and chromium in the mixed system onto the samples heat treated at different temperatures were investigated. The adsorption equilibrium of amoxicillin and chromium on the prepared activated carbons was reached after 180 min at 25°C. The initial concentration of amoxicillin and chromium were in the range of 40–300 and 0.5–3.75 mg/L, respectively.

The amount of amoxicillin or chromium adsorbed onto the prepared activated carbons at equilibrium (q_e in mg/g) was calculated as follows:

$$q_e = \frac{(C_0 - C_e)V}{m} \tag{1}$$

where C_0 and C_e are the initial dye concentration (mg/L) and the equilibrium dye concentration (mg/L), respectively; V is the volume of the solution (L) and m is the mass of the adsorbent (g).

The kinetics of amoxicillin and chromium adsorption in the mixed system onto the sample AC400 were investigated by varying the concentrations of the mixed amoxicillin and chromium at 50 and 0.625 mg/L; 100 and 1.25 mg/L; and 200 and 2.5 mg/L, respectively. The concentration of amoxicillin in aqueous solution was analyzed using a UV–Vis spectrophotometer (UV2800, China) at its maximum absorption wavelength of 272 nm. The amount of total chromium in aqueous solution was analyzed by an atomic absorption spectrometry (PEAA800, America).

3. Results and discussion

3.1. Characterization of the adsorbent

Table 1 shows the amounts of nitrogen, carbon and hydrogen contained in the activated carbon samples heat treated at the different temperatures. The findings demonstrate that the carbon contents increased from 63.00% to 74.69% with the increase of the heat treatment temperature. Furthermore, as the heat treatment temperature increased from 200°C to 400°C, the H/C was found to be decreased from 0.068 to 0.042, which indicates the enhanced carbonization and aromaticity [32]. The results, moreover, show that the elemental composition of the samples changed rapidly as the heating temperature reached 400°C. The sample AC400 contained the lowest amount of nitrogen (1.96%) and hydrogen (2.95%).

Fig. 1 shows the N_2 adsorption–desorption isotherms and pore size distribution curves of the samples at the various heat treatment temperatures. The isotherms of the sample AC200 are of type II in the IUPAC classification, which arises from nonporous or macroporous adsorbents. The isotherms of the sample AC300 have a hysteresis loop, indicating the development of mesoporosity (2–50 nm). The isotherms of the sample AC400 are of type IV with a hysteresis loop, which is characteristic of mesopores and slit-shaped pores. It can be seen from Fig. 1(b), the corresponding pore size distribution curves of the sample AC400 is around 10–30 nm. The isotherms of AC500 exhibit a type I with somewhat type IV character nitrogen isotherm, which have a rise at low relative pressure, indicating possibly the development of micropore volume because the sharp rise lied in the micropore filling, and a hysteresis loop indicated the mesopore [33]. From Fig. 1(b), the corresponding pore size distribution curves of AC500 are around 3–10 nm.

The BET surface area, total pore volume and external surface area of the samples heat treated at different temperatures are listed in Table 2. The BET surface area of the sample AC500 (514.57 m^2/g) is considerably larger than that of the sample AC200 (17.68 m^2/g) and AC300 (161.05 m^2/g). The BET surface area and micropore area increase greatly with the increasing activation temperature from 200°C to 500°C. The mesopore starts to develop at the temperature of 300°C. The sample AC400 with the activation temperature of 400°C has the largest mesopore volume as well as total pore volume. High mesopore development could be induced by phosphoric acid, which has been reported in other studies [34–36]. The mixture of pore sizes in the sample AC400 could be mainly produced by the activation of crystalline cellulose in the sample rather than amorphous polymers, which produces mostly micropores [37]. The results show that the surface area and porous structure are greatly influenced by the heat-treatment temperature for the prepared activated carbon.

Fig. 2 showed the surface and morphological characteristic of the seaweed before heat treated (a) and the sample AC400 (b). It can be seen in Fig. 2, the seaweed before heat treated has a typical fibrous morphology, and the morphology of sample AC400 is rigid and dense. The results indicated the surface of the seaweed was obviously changed after activation process.

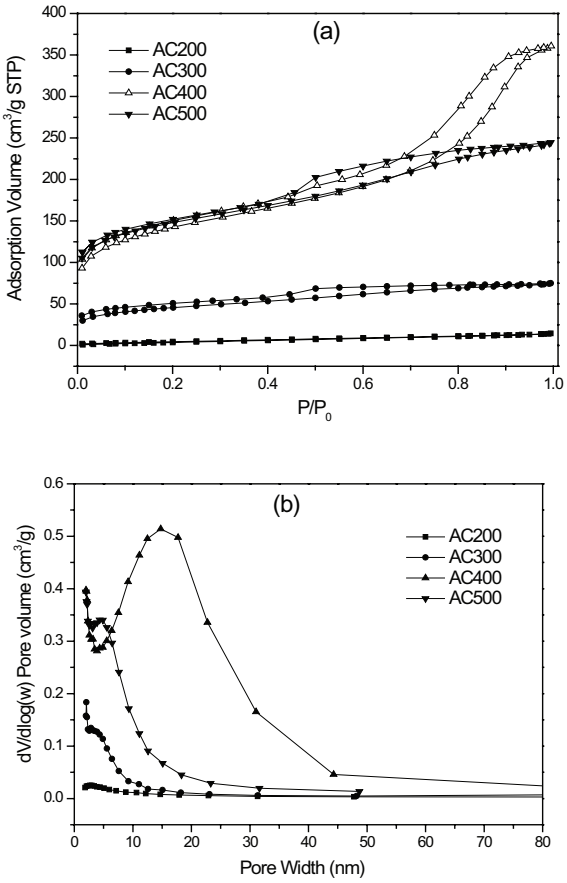

Fig. 1. N_2 adsorption–desorption isotherms (a) and pore size distribution curves of the samples (b) with different heat treatment temperature: AC200, AC300, AC400 and AC500.

Table 1
Elemental composition of the samples with different heat treatment temperature

Sample	N%	C%	H%	H/C
AC200	2.66	63.00	4.05	0.064
AC300	2.94	63.31	4.32	0.068
AC400	1.96	70.51	2.95	0.042
AC500	2.65	74.69	3.17	0.042

Table 2
BET surface area, total pore volume and external surface area of the samples

Samples	BET surface area, S_{BET} (m^2/g)	Micropore area (m^2/g)	Total pore volume (cm^3/g)	External surface area (m^2/g)	Mesopore volume (cm^3/g)
AC200	17.68	–	0.0210	29.45	–
AC300	161.05	49.66	0.1135	111.39	0.0917
AC400	500.18	166.81	0.5502	333.36	0.4759
AC500	514.57	231.95	0.3730	282.62	0.2678

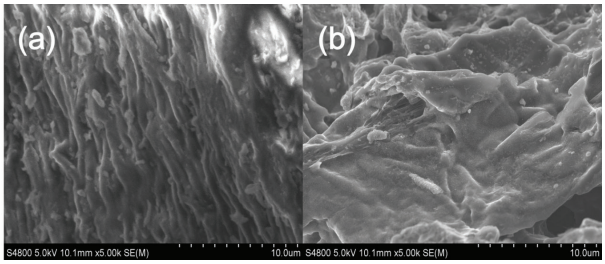

Fig. 2. The SEM images of seaweed before heat treated (a) and the sample AC400 (b).

3.2. Adsorption isotherms

Adsorption isotherms are commonly used to evaluate the performance of adsorbents in the adsorption process. They describe the interaction between adsorbates and adsorbents and also represent the surface properties of the adsorbent. The Freundlich adsorption model is used to fit the experimental data. The Freundlich model typical for heterogeneous surfaces is described as follows [38]:

$$q_e = K_F \cdot C_e^{\frac{1}{n}} \quad (2)$$

where K_F [(mg/g)(L/mg)$^{1/n}$] is the fitting affinity coefficient, and n is the Freundlich exponent related to adsorption intensity.

The isotherm parameters for the adsorption of amoxicillin and hexavalent chromium onto the samples are presented in Table 3. The Freundlich isotherms for the adsorption of amoxicillin (a) and hexavalent chromium (b) onto the samples of activated carbon produced at different heat treatment temperatures are shown in Fig. 3. For the adsorption of amoxicillin, the K_F of AC400 and AC500 determined as 6.6864 and 3.2191 (mg/g)(L/mg)$^{1/n}$ are considerably higher than that of AC200 and AC300, which were determined as 0.1831 and 0.1574. The adsorption capacities of AC400 and AC500 increased significantly in comparison with those of AC200 and AC300. The above results demonstrate that the AC400 and AC500 have significantly greater BET surface area and total pore volumes than the AC200 and AC300. In addition, the sample AC400, composed mainly of mesopore, has the largest total pore volume as well as adsorption capacity among all the samples. It is reported that the adsorption property of adsorbents is affected by the porous structure; the mesoporous structure could lead to less sterical hindrance and, thus, allow the easy diffusing of the substrate and molecules [39,40]. It can be concluded that the adsorption of amoxicillin onto the activated carbon in a binary solution with hexavalent chromium is highly dependent on the surface area and porous structure of the adsorbent. On the other hand, for the adsorption of hexavalent chromium, the K_F of AC200 and AC300 are significantly higher than that of the AC400 and AC500. The result showed that surface area and porous structure of the activated carbons have very limited effects on the adsorption of hexavalent chromium in binary solutions with amoxicillin.

Table 3
Adsorption isotherm parameters for the adsorption of amoxicillin and chromium onto the AC with different heat treatment temperature

Adsorbates	Adsorbents	Freundlich		
		K_F, (mg/g) (L/mg)$^{1/n}$	$1/n$	R^2
Amoxicillin	AC200	0.1831	0.9648	0.9971
	AC300	0.1574	0.9699	0.9978
	AC400	6.6864	0.3747	0.9611
	AC500	3.2191	0.4804	0.9805
Chromium	AC200	66.5658	1.6821	0.9166
	AC300	8.1630	1.2662	0.9874
	AC400	0.5754	2.9636	0.9271
	AC500	0.7287	1.8328	0.9315

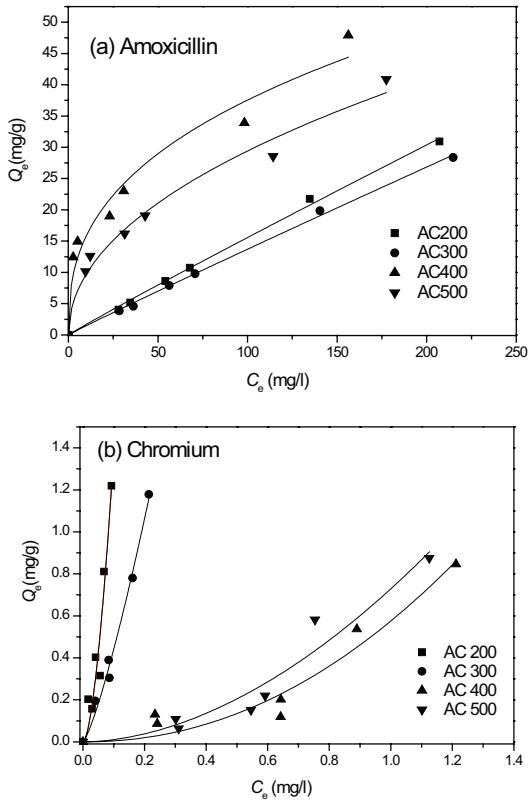

Fig. 3. Freundlich plot for adsorption of amoxicillin (a) and hexavalent chromium (b) onto the AC with different heat treatment temperature.

3.3. Adsorption kinetics

The pseudo-first-order and pseudo-second-order kinetic models were used to analyze the kinetics of amoxicillin and chromium adsorption onto the AC400. The pseudo-first-order model is described as follows [41]:

$$\ln(q_e - q_t) = \ln q_e - k_1 t \quad (3)$$

where q_e and q_t are adsorbate uptakes at equilibrium and time t (min), respectively, and k_1 is the pseudo-first-order rate constant (min^{-1}).

The pseudo-second-order model, based on the assumption of chemisorption, depicts the adsorption process properly [42]:

$$\frac{t}{q_t} = \frac{1}{k_2 q_e^{\,2}} + \frac{t}{q_e} \tag{4}$$

where k_2 is the pseudo-second-order rate constant [g(mg min)$^{-1}$].

Fig. 4 shows the pseudo-second-order kinetic curves for the adsorption of amoxicillin and chromium onto the AC400, respectively. The calculated kinetic rate constants, and experimental q_e values for the adsorption of amoxicillin and chromium at different initial concentrations onto the AC400 are presented in Table 4. Besides the correlation coefficients (R^2), the normalized standard deviation, Δq (%), was also calculated to quantitatively compare the applicability of each kinetic models.

$$\Delta q(\%) = 100 \times \sqrt{\frac{\sum[(q_{t,\exp} - q_{t,\mathrm{cal}})/q_{t,\exp}]^2}{(n-1)}} \tag{5}$$

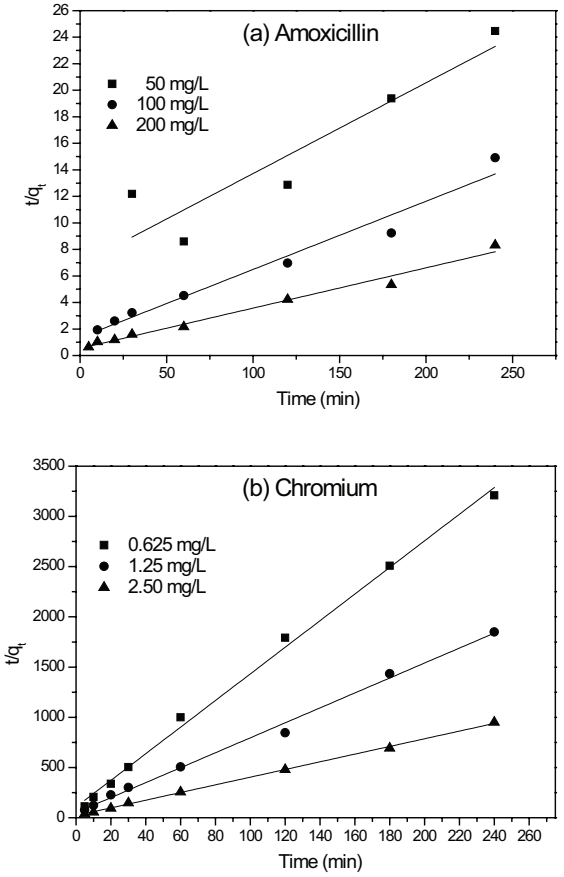

Fig. 4. Pseudo-second-order sorption kinetics of amoxicillin (a) and hexavalent chromium (b) onto the AC400.

The adsorption of amoxicillin fitted well to both the pseudo-first-order and pseudo-second-order kinetic models (R^2 > 0.9). According to the Table 4, the q_e calculated from this model is closer to the experimental q_e. And the Δq values from the pseudo-second-order model were found to be much lower than the pseudo-first-order kinetic model for the amoxicillin adsorption process. Therefore, the pseudo-second-order kinetic model could be more applicable to the amoxicillin adsorption process.

As shown in Table 4, the chromium experimental data exhibit much better fit to the pseudo-second-order kinetic model (R^2>0.99), which indicated that the process of chromium adsorption onto the AC400 could be chemisorption. The k_2 values for the adsorption of both amoxicillin and chromium onto the AC400 decreased with the increase of the initial concentrations. The increase in the initial amoxicillin and chromium concentrations could lead to the increasing of the driving force due to the improving of mass transfer rate [43].

3.4. The effect of pH

The pH_{pzc} is defined as the pH value at which the adsorbent surface acquires a neutral charge. It is an important factor for the adsorption process [44]. The pH_{pzc} was determined from the plot of ΔpH [$pH_{initial} - pH_{final}$] vs. $pH_{initial}$ (Fig. 5). The observed pH_{pzc} for the AC400 sample was 4.05, implying that the solid surface is positively charged at the solution pH < 4.05, negatively charged when the solution pH > 4.05, and neutral charged at the solution pH of 4.05.

The solution pH of amoxicillin and hexavalent chromium after adding the AC400 all showed a decrease compared with the original pH (in Fig. 6), which could be attributed to the effect of strongly acidic groups on the surface of AC400 [45]. The result indicated that the adsorbent caused a significant increase in the acidity of the mixed amoxicillin and hexavalent solutions.

The effects of the initial solution pH on the adsorption of amoxicillin and hexavalent chromium in the mixed system onto the AC400 are shown in Figs. 7(a) and (b), respectively. Fig. 7(a) demonstrated that the adsorption of amoxicillin onto the AC400 was rapid at the initial stage, which increased with the increase in solution pH from 4.0 to 7.9. The amoxicillin can exist in different forms in aqueous solution due to the ionization of its three functional groups, which can be identified as carboxyl (pK_{a1}: 2.68), amine (pK_{a2}: 7.49) and phenolic hydroxyl (pK_{a3}: 9.63) [46]. When the solution pH is lower than the pK_{a1}, the functional groups will be protonated as –COOH/–NH_3^+/–OH (amoxicillin$^+$); when the solution pH is between pK_{a1} and pK_{a2}, the carboxylic group will be deprotonated –COO^-/–NH_3^+/–OH (amoxicillin$^\pm$); at solution pH between pK_{a2} and pK_{a3}, both of the carboxylic and amine groups can be deprotonated –COO^-/–NH_2/–OH (amoxicillin$^-$) [43,47]. Therefore, the predominant amoxicillin species in the amoxicillin and hexavalent chromium mixed solution at pH range from 4.0 to 7.9 could be amoxicillin$^+$ and amoxicillin$^\pm$ species. From Fig. 6, after adding AC400 sample, the initial pH range from 4.0 to 5.0 of the mixed solution all decreased to around 3.0, in which the AC400 sample (pH_{pzc} = 4.05) was positive charged and both amoxicillin$^+$ and amoxicillin$^\pm$ species existed. Hence, the adsorption of amoxicillin onto AC400 sample was inhibited to a certain

Table 4
Pseudo-first-order and pseudo-second-order kinetic parameters for the adsorption of amoxicillin and chromium onto the AC400

Mixed contaminants concentration (mg/L)		q_e (mg/g)	Pseudo-first-order				Pseudo-second-order			
Amoxicillin	Chromium		k_1 (min^{-1})	q_e (cal) (mg/g)	R^2	Δq (%)	k_2 (g/mg min)	q_e (cal) (mg/g)	R^2	Δq (%)
			Kinetics for amoxicillin							
50	0.625	9.29	0.0235	11.25	0.862	78.5	0.00683	14.60	0.813	22.6
100	1.25	19.50	0.0198	19.25	0.935	17.7	0.00196	19.44	0.964	9.5
200	2.50	33.72	0.0278	31.70	0.987	13.5	0.00170	32.95	0.982	11.2
			Kinetics for chromium							
50	0.625	0.0718	0.0242	0.0346	0.459	73.4	1.6344	0.0755	0.996	15.3
100	1.25	0.1255	0.0424	0.0881	0.938	49.2	1.0758	0.1343	0.995	9.2
200	2.50	0.2597	0.0329	0.1500	0.743	62.1	0.6769	0.2615	0.999	4.8

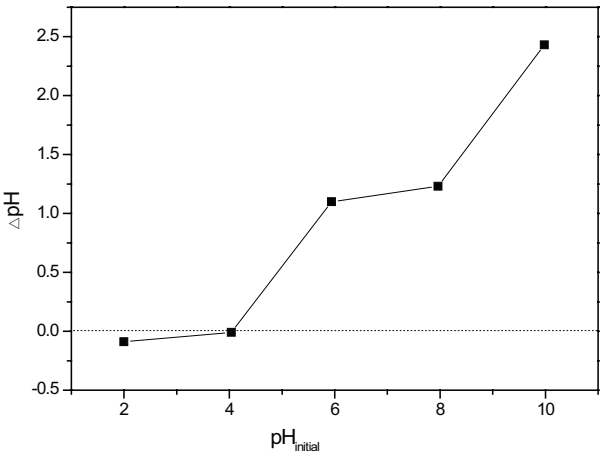

Fig. 5. Curve of the point zero charge (pH_{pzc}) of the AC400.

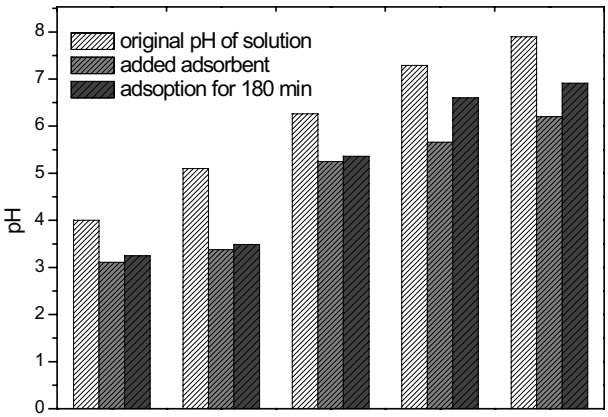

Fig. 6. The pH change of the solutions after adding the AC400 and adsorption for amoxicillin and hexavalent chromium onto the AC400 for 180 min.

extent at the initial solution pH range from 4.0 to 5.0 due to the electrostatic repulsion. While at the initial solution pH range from 5.0 to 7.9, the AC400 surface was negative charged, and the main amoxicillin group was amoxicillin$^{\pm}$, and the effect of electrostatic repulsion diminished. There are many mechanisms that could be involved in the adsorption of amoxicillin on the surface of AC400 sample, including electrostatic interaction, hydrogen bonding formation, electron donor–acceptor and π–π dispersion [48].

Fig. 7(b) shows the effect of the initial solution pH on the adsorption of hexavalent chromium in the mixed system onto the AC400. Hexavalent chromium species could exist in various forms in solution at different pH, such as H_2CrO_4, $HCrO_4^-$, $Cr_2O_4^{2-}$ and $Cr_2O_7^{2-}$. The equilibrium reactions involving these species are given in Eq. (6)–(8) [49,50]:

$$H_2CrO_4 \rightleftharpoons H^+ + HCrO_4^- \quad (6)$$

$$HCrO_4^- \rightleftharpoons H^+ + CrO_4^{2-} \quad (7)$$

$$2HCrO_4^- \rightleftharpoons Cr_2O_7^{2-} + H_2O \quad (8)$$

Based on thermodynamic database listed in Butler [49] and Stumm and Morgan [50], the distribution diagram of Cr(VI) species in water under different pH and total Cr(VI) concentration is shown in Fig. 8. As seen from Fig. 8, $HCrO_4^-$ and CrO_4^{2-} are the two major species in the solution at the experimental total Cr(VI) concentration. For pH lower than 6.3, $HCrO_4^-$ is the dominant species of Cr(VI), and above pH 7.3, only CrO_4^{2-} is stable. For hexavalent chromium (Fig. 7(b)), at the initial adsorption stage (within 10 min) the amount adsorbed onto the AC400 increased from 0.85 to 1.18 mg/g when the solution pH decreased from 7.9 to 4.0. At lower solution pH, the degree of protonation of the adsorbent surface is enhanced, which favors the adsorption of anionic form chromium, such as $HCrO_4^-$ and CrO_4^{2-}, onto the surface of the adsorbent [51]. While then at the gradual adsorption stage, the adsorption of hexavalent chromium onto the AC400 was obviously suppressed and showed somewhat decrease within pH 4.0–5.1. This result could be attributed to the carboxylate ($-COO^-$) that is dissociated from the amoxicillin molecule in solution to compete with the $HCrO_4^-$ for adsorption sites on the surface of the adsorbent and, thus, cause an obvious suppression for the adsorption of hexavalent chromium onto the AC400 [43]. Furthermore, the amoxicillin molecule

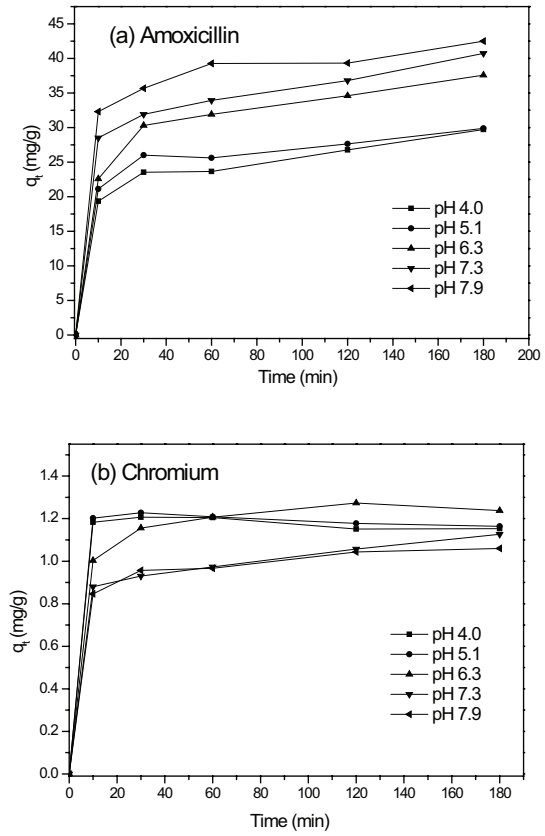

Fig. 7. The adsorption amount of amoxicillin (a) and hexavalent chromium (b) onto the AC400 with different pH.

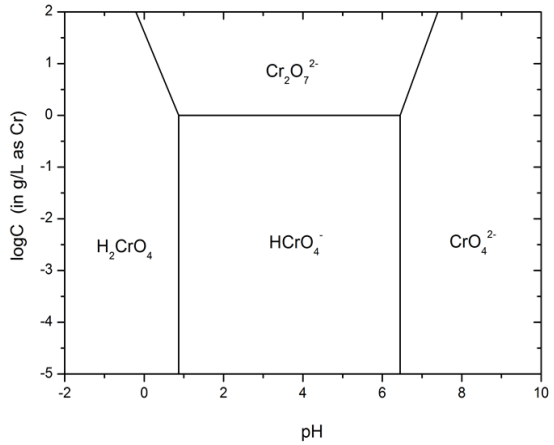

Fig. 8. The distribution diagram of Cr(VI) species in aqueous solution under different pH and total Cr(VI) concentration.

would be dissociated to amine and H^+ at pH around 6–8, which could favor the adsorption of hexavalent chromium onto the adsorbent [52]. As shown in Fig. 7(b), there is no decreasing trend for the adsorption of hexavalent chromium at the gradual adsorption stage at the pH range of 6.3–7.9. The optimum pH could be 6.3 for the adsorption of hexavalent chromium in the mixed system containing amoxicillin and hexavalent chromium onto the AC400.

4. Conclusions

Activated carbon from the seaweed kelp was synthesized by phosphoric acid activation and used as an adsorbent for the coadsorption of antibiotic amoxicillin and hexavalent chromium from saline water. The analysis of the elemental composition of the samples, which were heat treated at different temperatures, indicated that the carbonization and aromaticity increased rapidly with increasing temperature from 200°C to 400°C. N_2 adsorption–desorption isotherms indicated that the surface area and porous structure of the prepared activated carbons are greatly influenced by the heat-treatment temperature. The sample AC400 with the activation temperature of 400°C has the largest mesopore volume as well as total pore volume. The Freundlich isotherms for the adsorption of amoxicillin and chromium onto the prepared activated carbon from seawater were analyzed. For amoxicillin, the adsorption capacities of the samples AC400 and AC500 were significantly higher than that of AC200 and AC300; for hexavalent chromium, it is the opposite. The adsorption of amoxicillin fitted well to both the pseudo-first-order and pseudo-second-order kinetic models ($R^2 > 0.9$). The chromium experimental data exhibited much better fit to the pseudo-second-order kinetic model ($R^2 > 0.99$). The process of chromium adsorption onto the AC400 could be chemisorption. The optimum pH could be 6.3 for the adsorption of hexavalent chromium onto the AC400 in the mixed system containing amoxicillin and hexavalent chromium.

Acknowledgments

This work was supported by Ningbo Natural Science Foundation (2014A610093), Ningbo Science and Technology Plan Projects (2014C50007) and National Spark Program (2014GA701006).

References

[1] H.S. Fida, S. Guo, G.K. Zhang, Preparation and characterization of bifunctional Ti–Fe kaolinite composite for Cr(VI) removal, J. Colloid Interface Sci., 442 (2015) 30–38.
[2] I. Akcali, F. Kucuksezgin, A biomonitoring study: heavy metals in macroalgae from eastern Aegean coastal areas, Mar. Pollut. Bull., 62 (2011) 637–645.
[3] K. Pan, W.X. Wang, Trace metal contamination in estuarine and coastal environments in China, Sci. Total Environ., 421–422 (2012) 3–16.
[4] E.K. Putra, R. Pranowo, J. Sunarso, N. Indraswati, S. Ismadji, Performance of activated carbon and bentonite for adsorption of amoxicillin from wastewater: mechanisms, isotherms and kinetics, Water Res., 43 (2009) 2419–2430.
[5] C.C. Jara, D. Fino, V. Specchia, G. Saracco, P. Spinelli, Electrochemical removal of antibiotic from wastewaters, Appl. Catal., B, 70 (2007) 479–487.
[6] X. Pan, C. Deng, D. Zhang, J. Wang, G. Mu, Y. Chen, Toxic effects of amoxicillin on the photosystem II of *Synechocystis* sp. characterized by a variety of in vivo chlorophyll fluorescence tests, Aquat. Toxicol., 89 (2008) 207–213.
[7] W.W. Tang, G.M. Zeng, J.L. Gong, Y. Liu, X.Y. Wang, Y.Y. Liu, Z.F. Liu, L. Chen, X.R. Zhang, D.Z. Tu, Simultaneous adsorption of atrazine and Cu (II) from wastewater by magnetic multi-walled carbon nanotube, Chem. Eng. J., 211–212 (2012) 470–478.
[8] C. Leodopoulos, D. Doulia, K. Gimouhopoulos, T.M. Triantis, Single and simultaneous adsorption of methyl orange and humic acid onto bentonite, Appl. Clay Sci., 70 (2012) 84–90.

[9] M.F.N. Secondes, V. Naddeo, F. Ballesteros, Jr., V. Belgiorno, Adsorption of emerging contaminants enhanced by ultrasound irradiation, Sustain. Environ. Res., 24 (2014) 349–355.
[10] S. Babel, T.A. Kurmiawan, Low-cost adsorbents for heavy metals uptake from contaminated water: a review, J. Hazard. Mater., *97* (2003) 219–243.
[11] B.L. Chen, D.D. Zhou, L.Z. Zhu, Transitional adsorption and partition of nonpolar and polar aromatic contaminants by biochars of pine needles with different pyrolytic temperatures, Environ. Sci. Technol., 42 (2008) 5137–5143.
[12] R.T. Wang, P.Y. Wang, X.B. Yan, J.W. Lang, C. Peng, Q.J. Xue, Promising porous carbon derived from celtuce leaves with outstanding supercapacitance and CO_2 capture performance, ACS Appl. Mater. Interfaces, 4 (2012) 5800–5806.
[13] Y. Yang, Y.Q. Zhao, A.O. Babatunde, L. Wang, Y.X. Ren, Y. Han, Characteristics and mechanisms of phosphate adsorption on dewatered alum sludge, Sep. Purif. Technol., 51 (2006) 193–200.
[14] A.O. Babatunde, Y.Q. Zhao, Equilibrium and kinetic analysis of phosphorus adsorption from aqueous solution using waste alum sludge, J. Hazard. Mater., 184 (2010) 746–752.
[15] Y. Yang, Y.Q. Zhao, A.O. Babatunde, L. Wang, Y.X. Ren, Y. Han, Preparation and characteristics of rice-straw-based porous carbons with high adsorption capacity, Sep. Purif. Technol., 51 (2006) 193–200.
[16] A.T. Mohd Din, B.H. Hameed, A.L. Ahmad, Batch adsorption of phenol onto physiochemical-activated coconut shell, J. Hazard. Mater., 161 (2009) 1522–1529.
[17] M.J. Ahmed, S.K. Theydan, Equilibrium isotherms, kinetics and thermodynamics studies of phenolic compounds adsorption on palm-tree fruit stones, Ecotoxicol. Environ. Saf., 84 (2012) 39–45.
[18] P. Senthil Kumar, S. Ramalingam, C. Senthamarai, M. Niranjanaa, P. Vijayalakshmi, S. Sivanesan, Adsorption of dye from aqueous solution by cashew nut shell: studies on equilibrium isotherm, kinetics and thermodynamics of interactions, Desalination, 261 (2010) 52–60.
[19] C.L. Wang, D. Ma, X.H. Bao, Transformation of biomass into porous graphitic carbon nanostructures by microwave irradiation, J. Phys. Chem. C, 112 (2008) 17596–17602.
[20] A.A. Hamdy, Biosorption of heavy metals by marine algae, Curr. Microbiol., 41 (2000) 232–238.
[21] E. Valdman, L. Erijman, F.L.P. Pessoa, S.G.F. Leite, Continuous biosorption of Cu and Zn by immobilized waste biomass *Sargassum* sp., Process Biochem., 36 (2001) 869–873.
[22] S.S. Baral, N. Das, G. Roy Chaudhury, S.N. Das, A preliminary study on the adsorptive removal of Cr(VI) using seaweed, *Hydrilla verticillata*, J. Hazard. Mater., 171 (2009) 358–369.
[23] A. El-Sikaily, A. El Nemr, A. Khaled, O. Abdelwehab, Removal of toxic chromium from wastewater using green alga *Ulva lactuca* and its activated carbon, J. Hazard. Mater., 148 (2007) 216–228.
[24] A. Rathinam, J.R. Rao, B.U. Nair, Adsorption of phenol onto activated carbon from seaweed: determination of the optimal experimental parameters using factorial design, J. Taiwan Inst. Chem. Eng., 42 (2011) 952–956.
[25] Y. Ngernyen, C. Tangsathitkulchai, M. Tangsathitkulchai, Porous properties of activated carbon produced from Eucalyptus and Wattle wood by carbon dioxide activation, Korean J. Chem. Eng., 23 (2006) 1046–1054.
[26] A. Ahmadpour, D.D. Do, The preparation of active carbons from coal by chemical and physical activation, Carbon, 34 (1996) 471–479.
[27] D. Prahas, Y. Kartika, N. Indraswati, S. Ismadji, Activated carbon from jackfruit peel waste by H_3PO_4 chemical activation: pore structure and surface chemistry characterization, Chem. Eng. J., 140 (2008) 32–42.
[28] M. Benadjemia, L. Millière, L. Reinert, N. Benderdouche, L. Duclaux, Preparation, characterization and Methylene Blue adsorption of phosphoric acid activated carbons from globe artichoke leaves, Fuel Process. Technol., 92 (2011) 1203–1212.
[29] P. Patnukao, P. Pavasant, Activated carbon from *Eucalyptus camaldulensis Dehn* bark using phosphoric acid activation, Bioresour. Technol., 99 (2008) 8540–8543.
[30] E.P. Barret, L.G. Joyer, P.P. Halenda, The determination of pore volume and area distribution in porous substances. I. Computations from nitrogen isotherms, J. Am. Chem. Soc., 73 (1951) 373–378.
[31] B.C. Lippens, J.H. de Boer, Studies on pore systems in catalysts. V. The *t* method, J. Catal., 4 (1965) 319–325.
[32] Y. Chun, G.Y. Sheng, C.T. Chiou, B.S. Xing, Compositions and sorptive properties of crop residue-derived chars, Environ. Sci. Technol., 38 (2004) 4649–4655.
[33] Q.B. Wen, C.T. Li, Z.Z. Cai, W. Zhang, H.L. Gao, L.J. Chen, G.M. Zeng, X. Shu, Y.P. Zhao, Study on activated carbon derived from sewage sludge for adsorption of gaseous formaldehyde, Bioresour. Technol., 102 (2011) 942–947.
[34] H. Teng, T.S. Yeh, L.H. Hsu, Preparation of activated carbon from bituminous coal with phosphoric acid activation, Carbon, 36 (1998) 1387–1395.
[35] S. Timur, I.C. Kantarli, E. Ikizoglu, J. Yanik, Preparation of activated carbons from oreganum stalks by chemical activation, Energy Fuels, 20 (2006) 2636–2641.
[36] J. Laine, A. Calafat, M. Labady, Preparation and characterization of activated carbons from coconut shell impregnated with phosphoric acid, Carbon, 27 (1989) 191–195.
[37] M. Jagtoyen, F. Derbyshire, Activated carbons from yellow poplar and white oak by H_3PO_4 activation, Carbon, 36 (1998) 1085–1097.
[38] H.M.F. Freundlich, About the adsorption in solutions, J. Phys. Chem., Leipzig, 57 (1906) 385–470.
[39] Y.H. Li, S.G. Wang, Z.K. Luan, J. Ding, C.L. Xu, D.H. Wu, Adsorption of cadmium(II) from aqueous solution by surface oxidized carbon nanotubes, Carbon, 41 (2003) 1057–1062.
[40] Y.H. Deng, Y. Cai, Z.K. Sun, J. Liu, C. Liu, J. Wei, W. Li, C. Liu, Y. Wang, D.Y. Zhao, Multifunctional mesoporous composite microspheres with well-designed nanostructure: a highly integrated catalyst system, J. Am. Chem. Soc., 132 (2010) 8466–8473.
[41] Y.S. Ho, G. McKay, Sorption of dye from aqueous solution by peat, Chem. Eng. J., 70 (1998) 115–124.
[42] Y.S. Ho, G. McKay, Pseudo-second order model for sorption processes, Process Biochem., 34 (1999) 451–465.
[43] G. Moussavi, A. Alahabadi, K. Yaghmaeian, M. Eskandari, Preparation, characterization and adsorption potential of the NH_4Cl-induced activated carbon for the removal of amoxicillin antibiotic from water, Chem. Eng. J., 21 (2013) 119–128.
[44] G. Asgari, B. Ramavandi, L. Rasuli, M. Ahmadi, Cr (VI) adsorption from aqueous solution using a surfactant-modified Iranian zeolite: characterization, optimization, and kinetic approach, Desal. Wat. Treat., 51 (2013) 6009–6020.
[45] J.W. Shim, S.J. Park, S.K. Ryu, Effect of modification with HNO and NaOH on metal adsorption by pitch-based activated carbon fibers, Carbon 39 (2001) 1635–1642.
[46] A.F. Goddard, M.J. Jessa, D.A. Barrett, P.N. Shaw, J.P. Idstrom, C. Cederberg, R.C. Spiller, Effect of omeprazole on the distribution of metronidazole, amoxicillin, and clarithromycin in human gastric juice, Gastroenterology, 111 (1996) 358–367.
[47] E.K. Putra, R. Pranowo, J. Sunarso, N. Indraswati, S. Ismadji, Performance of activated carbon and bentonite for adsorption of amoxicillin from wastewater: mechanisms, isotherms and kinetics, Water Res., 43 (2009) 2419–2430.
[48] A.C. Martins, O. Pezoti, A.L. Cazetta, K.C. Bedin, D.A.S. Yamazaki, G.F.G. Bandoch, T. Asefa, J.V. Visentainer, V.C. Almeida, Removal of tetracycline by NaOH-activated carbon produced from macadamia nut shells: kinetic and equilibrium studies, Chem. Eng. J., 260 (2015) 291–299.
[49] J.N. Butler, Ionic Equilibrium, Addison-Wesley, New York, 1967.
[50] W. Stumm, J.J. Morgan, Aquatic Chemistry: An Introduction Emphasizing Chemical Equilibria in Natural Waters, John Wiley & Sons, Inc., New York, 1996.
[51] K. Selvi, S. Pattabhi, K. Kadirvelu, Removal of Cr(VI) from aqueous solution by adsorption onto activated carbon, Bioresour. Technol., 80 (2001) 87–89.
[52] R. Andreozzi, M. Canterino, R. Marotta, N. Paxeus, Antibiotic removal from wastewaters: the ozonation of amoxicillin, J. Hazard. Mater., 122 (2005) 243–250.